催化学报
2011 Chinese Journal of Catalysis Vol. 32 No. 3

文章编号: 0253-9837(2011)03-0451-05 国际版 DOI: 10.1016/S1872-2067(10)60197-0 研究论文: 451~455

在预吸附氧原子的Ag(100)面上氯乙烯环氧化反应的密度泛函理论研究

吕永康[1], 郗瑞鑫[1], 任瑞鹏[1,2]

[1]太原理工大学煤科学与技术教育部与山西省重点实验室, 山西太原030024

[2]太原理工大学化学化工学院, 山西太原030024

摘要: 采用密度泛函理论和周期性平板模型对氯乙烯在预吸附氧原子的Ag(100)面上选择性环氧化反应进行了模拟计算. 结果表明, 该反应首先由反应物生成中间体, 再由中间体生成产物. 由于氯乙烯是一种不对称的分子, 所以该反应存在两种可能的途径. 比较反应活化能可以发现, 在一个反应通道中环氧氯乙烷要比氯乙醛的生成更容易; 而在另一反应通道中, 氯乙醛要易于环氧氯乙烷和乙酰氯的生成. 同时还研究了中间体中碳原子和银原子的投影态密度 (PDOS), 以期更深入地了解两种不同反应途径活化能差异的原因.

关键词: 氯乙烯; 密度泛函理论; 选择性环氧化; 银; 预吸附; 氧原子

中图分类号: O643 **文献标识码:** A

Vinyl Chloride Selectivity during Epoxidation on Oxygen Pre-adsorbed Ag(100): A Density-Functional Theory Study

LÜ Yongkang[1,*], XI Ruixin[1], REN Ruipeng[1,2]

[1]*Key Laboratory of Coal Science and Technology, Ministry of Education and Shanxi Province, Taiyuan University of Technology, Taiyuan 030024, Shanxi, China*

[2]*College of Chemistry and Chemical Engineering, Taiyuan University of Technology, Taiyuan 030024, Shanxi, China*

Abstract: Vinyl chloride selectivity during epoxidation on an atomic oxygen pre-adsorbed Ag(100) surface using density functional theory (DFT) with the periodic slab model was investigated. The reaction mechanism is a two-step process where chloroethylene oxametallacycle intermediate (OMMC) is first formed and then converted to the products. Because of the asymmetry of vinyl chloride, two competitive reaction pathways are evident. The reaction energies and the activation energies of the processes were determined by the DFT calculations. Compared with the reaction activity energy, in one pathway the formation of chloroethylene epoxide (CE) is more favorable than the formation of chloroacetaldehyde (CA) whereas in the other pathway, the formation of CA is more favorable than the formation of CE and acetyl chloride. To further understand the reason for the selectivity difference in these different paths the projected density of states of the C atom and the Ag atom involved in the OMMC was calculated.

Key words: vinyl chloride; density functional theory; selectivity epoxidation; silver; pre-adsorption; oxygen

The epoxidation of alkenes is a technologically relevant reaction because epoxides are versatile intermediates during chemical synthesis. Ethylene oxide (EO) is especially known to be largely converted into ethylene glycol as well as many other derivatives and has long been one of the highest volume chemicals produced by the chemical industry. It accounts for approximately 40%–50% of the total value of organic chemicals produced by heterogeneous oxidation [1–3]. As a major petrochemical process, ethylene epoxidation by selective oxidation has attracted much attention. Much research has been directed toward establishing the reaction mechanism of ethylene epoxidation. For epoxidation reactions occurring on Ag(111) surfaces, and even for partially oxidized silver surfaces, the molecular mechanism is known in detail [4–6] and is generally: $C_2H_4 + O \rightarrow$ oxametallacycle (OMME) $\rightarrow C_2H_4O/CH_3CHO$. In another

Received 25 November 2010. Accepted 29 December 2010.

***Corresponding author.** Tel: +86-25-83686219; Fax: +86-25-83686251; E-mail: lykang@tyut.edu.cn

English edition available online at ScienceDirect (http://www.sciencedirect.com/science/journal/18722067).

words, this mechanism involves the reaction of ethylene with adsorbed oxygen through a partial oxidation route to form either EO or acetaldehyde from an OMME intermediate [2]. Transient surface experiments such as temperature-programmed reactions (TPR) and pulse experiments combined with different surface characterization tools (X-ray photoelectron spectroscopy (XPS), ultraviolet photoelectron spectroscopy (UPS), atomic emission spectrometry (AES), etc.) have been used to advance our understanding of ethylene epoxidation. These experiments indicate that the atomic oxygen on silver is more active than molecular oxygen [7–11]. As mentioned above, it is generally recognized that Ag is an efficient catalyst for these reactions based on experimental results as well as recent theoretical calculations.

Although numerous studies exist in the literature regarding the transformation of ethylene to EO on silver [4,5,8,11,12], the detailed selective oxidation mechanism for asymmetric molecules is inadequate [3,13]. In this article, we pay attention to the partial oxidation of vinyl chloride (VC) on the surface of Ag(100). Ag(100) is considered to be a perfect substrate and it has a face-centered cubic structure, low ligancy, and high symmetry. We used VC in this work because it is chemically analogous in reactivity to ethylene and the chemical effects after hydrogen substitution by chlorine may be analyzed. We thus present a periodic density functional study of the epoxidation mechanism of VC on an oxygen pre-adsorbed metal surface of Ag(100).

1 Calculation methods and models

A mechanism for VC epoxidation has been previously investigated by first-principles calculations based on density functional theory (DFT) applied to slab models representing the Ag(100) surface pre-adsorbed with O atoms. Slab models have also been used for adsorption calculations [14]. All the calculations were carried out using the Vienna ab initio simulation package (VASP) code [15–17]. To model the metal surfaces, a periodic array model containing four atomic layers with a full relaxation of the first two layers was used and the slabs were separated by a ~1.5 nm vacuum region. A p(2×2)-unit cell was chosen, which means a monolayer of adsorbates was present with a 1/4 monolayer (ML) coverage. In our calculations, a Monkhorst-Pack mesh of a 3×3×1 special k-point was used for integration into the surface Brillouin zone. The project-augment wave (PAW) method was used to describe the inner cores, and the electronic wave functions of the valence electrons were expanded on a plane wave basis with a kinetic energy cutoff of 400 eV [15]. The exchange-correlation functional used to obtain the energy was the Perdew-Wang (PW91) implementation of the generalized gradient approach [18,19]. The climbing-nudged elastic band method (cNEB) [20,21] was used to locate the transition state (TS). A frequency analysis was performed to confirm the TS. In this work, the activation energy (E_a) was calculated according to $E_a = E_{TS/M} - E_{reactant/M}$, where $E_{TS/M}$ is the calculated total energy without the entropy of the TS, and $E_{reactant/M}$ is the calculated total energies without the entropy of the reactant before the corresponding TS. For reactions like AB = A + B, the heats of reaction (or total energy change) ΔE are calculated by $\Delta E = E_{(A+B)/M} - E_{AB/M}$ (where $E_{(A+B)/M}$ is the total energy for the A+B+M co-adsorption system).

2 Results and discussion

First, the VC molecule and the oxygen atom were optimized over the Ag(100) substrate. The optimized results are shown in Fig. 1. From Fig. 1, after optimization the VC molecule is on the bridge site and the O atom is on the 4h site. The other species of interest in this process were also optimized and are shown in Fig. 1. The reaction mechanism is: C_2H_3Cl + O → OMMC → $C_2H_3ClO/CH_3CClO/CH_2ClCHO$, which is illustrated in Fig. 2 and is analogous

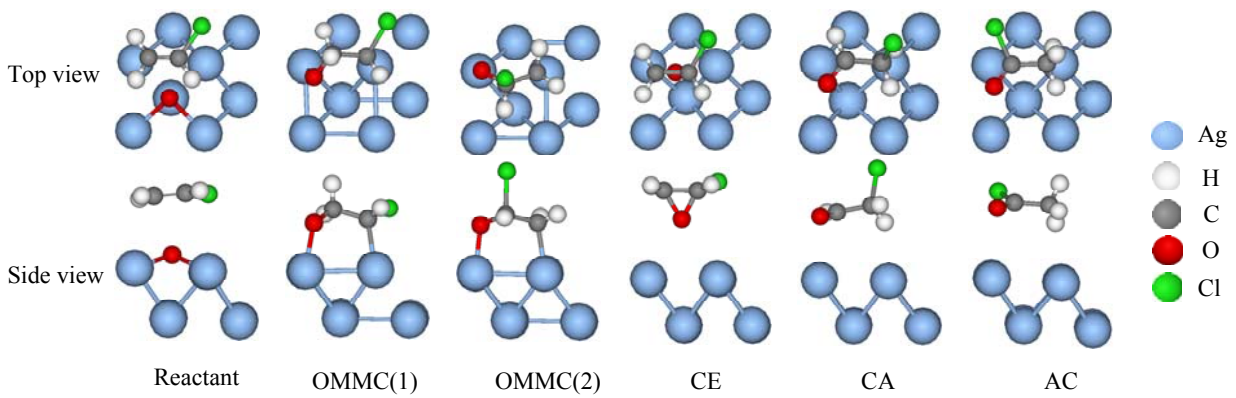

Fig. 1. Top and side view of the structures of reactants (VC and oxygen atom) during epoxidation for products (CE, CA, AC) on Ag (100). CE: chloroethylene epoxide; CA: chloroacetaldehyde; AC: acetyl chloride.

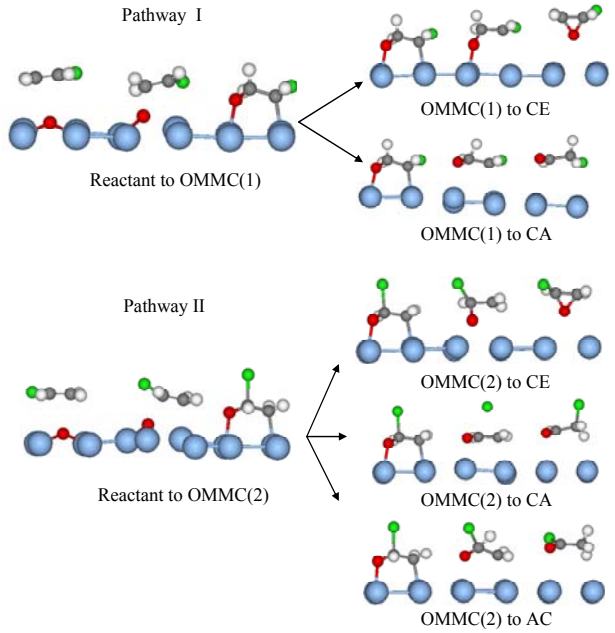

Fig. 2. Competitive reaction for the VC oxidation reaction on Ag(100).

with the mechanism proposed previously [3–5]. Because VC is asymmetric, the OMMCs are labeled OMMC(1) and OMMC(2) while the Cl atom is in a different position, as shown in Fig. 1. In the OMMCs, the carbon in the VC connected to O is designated C_1 and the neighboring carbon is C_2. The related bond distances are listed in Table 1. After optimization, all the OMMC structures are of the closed-ring type, which is in accordance with the closed-ring OMME structures proposed in a previous study on ethylene epoxidation on Cu(111) [22].

Because of the two different OMMC structures there are two possible reaction pathways. The products are determined by the different reaction pathways, as shown in Fig. 2. For reaction pathway I, CE and CA are formed and the products are CE, CA, and AC in reaction pathway II.

After the initial states (IS) and final states (FS) of the reaction were optimized, saddle points were found in the minimum energy path using the cNEB method for each elementary step in the reaction mechanism. The likely TS structures produced by the cNEB method were further refined. The existence of a single normal mode associated with a pure imaginary frequency is a criterion for TS identification. All the TS structures were characterized by vibration frequency analysis. The results of the vibration frequency analysis are given in Table 2 together with the results of activity energy and reaction energy change.

Table 2 Reaction energy data from the DFT calculations of the two pathways for the reaction on the Ag(100) surface

Pathway	Reaction	E_a/eV	ΔE^a/eV	Imaginary frequency (cm^{-1})
I	to OMMC(1)	0.96	0.09	387.74
	to CA	1.28	−0.96	670.98
	to CE	1.02	−0.18	189.15
II	to OMMC(2)	0.94	−0.09	357.84
	to AC	1.00	−1.58	787.89
	to CE	0.86	0.01	340.38
	to CA	0.59	−0.80	210.95

[a]Total energy change.

2.1 OMMC formation

The two pathways are illustrated in Fig. 2. After the adsorption of VC and O atoms on the Ag(100) surface the TS structures were calculated using the minimum energy pathway that connected the IS and FS. The two processes are highly analogous. In this step, the O atom gradually moves to C_1 and finally bonds with C_1 and a Ag metal atom while the C_2 atom bonds with the Ag atom and the OMMC structures are formed. The optimized bond lengths of the TS structures during OMMC formation are summarized in Table 3. The bond length of C_1–O during the formation of the TS of OMMC(1) is 0.19 nm, and in the TS of OMMC(2) is 0.21 nm, respectively. We propose that the electronegativity of the chlorine atom may result in this phenomenon. The

Table 1 Bond distance (d) of the possible species (reactant, intermediate, and products) on the Ag(100) surface

Pathway	Species	d(O–M)/nm	d(C_1–M)/nm	d(C_2–M)/nm	d(C_1–C_2)/nm	d(C_1–O)/nm	d(C_2–O)/nm
I	VC	—	0.32	0.35	0.13	—	—
	oxygen	0.22	—	—	—	—	—
	OMMC(1)	0.21	0.29	0.22	0.15	0.14	0.24
	CA	0.34	0.34	0.36	0.15	0.12	0.24
	CE	0.30	0.39	0.40	0.15	0.15	0.14
II	VC	—	0.32	0.32	0.13	—	—
	oxygen	0.22	—	—	—	—	—
	OMMC(2)	0.21	0.30	0.22	0.15	0.13	0.24
	AC	0.32	0.34	0.34	0.15	0.12	0.24
	CE	0.27	0.38	0.37	0.15	0.14	0.14
	CA	0.29	0.31	0.34	0.15	0.12	0.24

Table 3 Bond distance of calculated TS structures for the possible elemental steps involved in the VC epoxidation on Ag in the calculated pathways

Pathway	TS	d(O–M)/nm	d(C_1–M)/nm	d(C_1–C_2)/nm	d(C_1–O)/nm	d(C_2–O)/nm
I	to OMMC(1)	0.22	0.31	0.14	0.19	0.27
	to CA	0.30	0.33	0.15	0.13	0.25
	to CE	0.21	0.32	0.15	0.14	0.24
II	to OMMC(2)	0.21	0.30	0.14	0.21	0.28
	to AC	0.26	0.32	0.15	0.13	0.25
	to CE	0.23	0.35	0.15	0.14	0.20
	to CA	0.23	0.25	0.14	0.13	0.24

interaction between the O and C_1 atoms can be weakened when the chlorine atom bonds with C_1. The active energies of this reaction step are 0.96 and 0.94 eV for the two processes (in Table 2).

2.2 CA, AC, and CE formation

CA can be produced via OMMC(1) and OMMC(2). A H shift process exists from OMMC(1) to CA. The H atom gradually moves to the C_2 atom and H–C_1 ruptures while the bond between C_2–Ag and O–Ag breaks down, a C_2–H bond forms and, therefore, CA is formed. The activity energy of this step is 1.28 eV and the exothermicity is 0.96 eV. In the pathway that yields CA via OMMC(2), Cl–C_1 is cleavaged and a Cl–C_2 bond forms. The O–Ag and C_2–M bonds break down simultaneously and then CA is produced. The activity energy of this step is 0.59 eV and the exothermicity is 0.80 eV.

AC can only be obtained in pathway II. The process of AC formation is just like CA formation in pathway I and it also has a H shift step. The activity energy of the TS structures for AC formation is 1.00 eV and the exothermicity is 1.58 eV.

The cyclization process during the formation of CE can progress via two OMMCs and the reaction steps are almost the same in the two pathways. This process includes breaking of the O–Ag and C_2–Ag bonds and the formation of a O–C_2 bond. From OMMC to CE, the C_2–Ag and O–Ag bonds break down and, simultaneously, the O atom gradually moves to the C_2 atom while the C_2–O bond forms and then CE forms. During the CE formation reaction the activity energy is 1.02 and 0.86 eV, and the exothermicity is 0.18 eV in pathway I. The endothermicity is 0.01 eV in pathway II.

2.3 Overview and comparison of the energy in different pathways

The reaction mechanism of this reaction is very different to the reaction of ethylene selection oxidation on a silver surface. For the epoxidation of ethylene, one pathway exists for the formation of EO and acetaldehyde [4–6]. However, in this reaction two competitive reaction pathways exist because of the asymmetry of the VC molecule. The process of VC epoxidation on Ag(100) surfaces occurs in two steps: (i) the VC and oxygen atom move together to produce the OMMCs; (ii) the OMMCs are catalyzed to form products via TSs.

Clearly, the activation barriers that characterize the competing reaction pathways on Ag play an important role in determining reaction selectivity and selectivity differences. The activation barriers on silver are 1.02 and 1.28 eV for CE and CA formation in pathway I and 0.86, 0.59, and 1.00 eV for CE, CA, and AC formation in pathway II, respectively. These barriers are higher than those in ethylene epoxidation: 0.80 and 0.73 eV [23]. Obviously, the formation of CE is less activated than CA formation in pathway I whereas in pathway II the formation of CA is less activated than the others. The difference in activation energy in the two pathways suggests that CE formation is more favorable in pathway I, however, in pathway II, CA formation is easier than that of AC and CE.

To further explore the possible reason for the above-mentioned difference the projected density of states (PDOS) of the C_2 atom involved in the OMMC was calculated. The carbon atom p band was compared with the metal d band for the OMMC (Fig. 3). The strength of the interaction between Ag and OMMC can be compared by the distance between the p band center of the C atom and the d band center of the Ag atom. The band center is calculated by the formula [24]:

$$\varepsilon^{c} = \int_{-\infty}^{E_f} E\rho(E)\mathrm{d}E \Big/ \int_{-\infty}^{E_f} \rho(E)\mathrm{d}E$$

where ρ represents the density of states projected onto the atom band and E_f is the Fermi energy. Figure 3 shows the density of states plot of the two OMMC systems. The distances between the p-band center and d-band center in the two routes are 0.50 and 0.72, respectively. This illustrates why the activation barriers of the formation of CE and CA in pathway I are higher than the activation barriers of formation of CE, CA, and AC in pathway II.

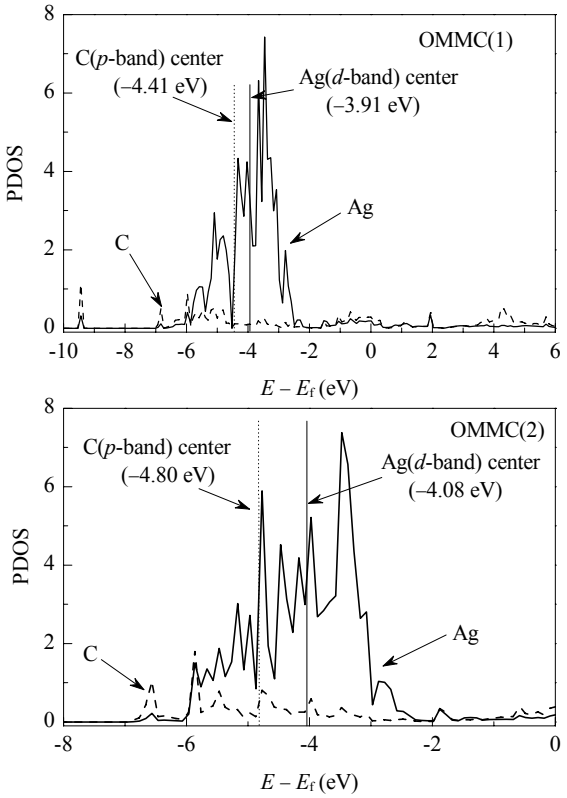

Fig. 3. PDOS for the carbon atom (*p*-band) and Ag(100) surface first layer atoms (*d*-band) of the OMMC. The lines denote the centers of the energy bands.

3 Conclusions

We undertook a DFT study to determine the possible vinyl chloride epoxidation process on an atomic oxygen pre-adsorbed Ag(100) surface. The reaction mechanism is a two-step process where OMMC forms and then the products form. By comparison with the reaction activity energy, in pathway I the formation of CE is more favorable than the formation of CA. In pathway II the route from OMMC(2) to CA is easier than the formation of CE and AC. Relative to Ag(111) [23], Ag(100) is different because of an inversion of the activation energy barrier for cyclization to CE versus a H-shift to CA in pathway I.

References

1 Jankowiak J T, Barteu M A. *J Catal*, 2005, **236**: 366
2 Torres D, Lopez N, Illas F. *J Catal*, 2006, **243**: 404
3 Pang X Y, Xing B, Xue L Q, Wang G C. *J Comput Chem*, 2010, **31**: 1618
4 Linic S, Barteau M A. *J Am Chem Soc*, 2003, **125**: 4034
5 Bocquet M L, Sautet P, Cerda J, Carlisle C I, Webb M J, King D A. *J Am Chem Soc*, 2003, **125**: 3119
6 Bocquet M L, Loffreda D. *J Am Chem Soc*, 2005, **127**: 17207
7 Van Santen R A, Kuipers H P C E. *Adv Catal*, 1987, **35**: 265
8 Grant R B, Lambert R M. *J Catal*, 1985, **92**: 364
9 Bukhtiyarov V I, Boronin A I, Prosvirin I P, Savschenko V I. *J Catal*, 1994, **150**: 268
10 Gleaves J T, Sault A G, Madix R J, Ebner J R. *J Catal*, 1990, **121**: 202
11 Stegelmann C, Stoltze P. *J Catal*, 2004, **226**: 129
12 Linic S, Piao H, Adib K, Barteau M A. *Angew Chem*, *Int Ed*, 2004, **43**: 2918
13 Torres D, Lopez N, Illas F, Lambert R M. *Angew Chem*, *Int Ed*, 2007, **46**: 2055
14 刘书红, 陈文凯, 曹梅娟, 许莹, 李俊箋. 催化学报 (Liu S H, Chen W K, Cao M J, Xu Y, Li J J. *Chin J Catal*), 2006, **27**: 55
15 Blochl P E. *Phys Rev B*, 1994, **50**: 17953
16 Kresse G, Joubert D. *Phys Rev B*, 1999, **59**: 1758
17 Morikawa Y, Iwata K, Terakur K. *Appl Surf Sci*, 2001, **169**: 11
18 White J A, Bird D M. *Phys Rev B*, 1994, **50**: 4954
19 Perdew J P, Chevary J A, Vosko S H, Jackson K A, Pederson M R, Singh D J, Fiolhais C. *Phys Rev B*, 1992, **46**: 6671
20 Mills G, Jonsson H, Schenter G K. *Surf Sci*, 1995, **324**: 305
21 Henkelman G, Uberuaga B P, Jonsson H. *J Chem Phys*, 2000, **113**: 9901
22 Linic S, Jankowiak J, Barteau M A. *J Catal*, 2004, **224**: 489
23 Torres D, Lopez N, Illas F, Lambert R M. *J Am Chem Soc*, 2005, **127**: 10774
24 Xing B, Pang X Y, Wang G C, Shang Z F. *J Mol Catal A*, 2010, **315**: 187